Stability of Rayleigh-stable Couette flow between two differentially heated cylinders

Antoine Meyer and Innocent Mutabazi*
Laboratoire Ondes et Milieux Complexes, Normandie Université, UNIHAVRE, CNRS UMR 6294, 53 rue de Prony, B.P. 540, F-76058 Le Havre Cedex, France

Harunori N. Yoshikawa
Université Côte d'Azur, CNRS, Institut de Physique de Nice, 06100 Nice, France

(Received 1 December 2020; accepted 2 March 2021; published 22 March 2021)

The stability of the circular Couette flow with two differentially heated cylinders is studied in the special cases of hydrodynamically stable rotation regimes. A one-dimensional model is developed to derive the condition of flow stability. This condition combines the curvature of the cylinders, the applied temperature difference between the two cylinders, and the diffusion properties of the fluid. The three-dimensional analysis is performed for two different rotation regimes: the Keplerian regime and the regime where the inner cylinder is stationary. The main results of this analysis is that, for a given radius ratio of the two cylinders, a single parameter combining the Prandtl number and the thermal expansion parameter can describe the critical state of the system. The description is in good agreement with the result of the one-dimensional model. An energy analysis shows a subtle role played by the shear stress in these two rotation regimes.

DOI: 10.1103/PhysRevFluids.6.033905

I. INTRODUCTION

The Taylor-Couette instability consists of the destabilization of the flow of a Newtonian fluid confined between two concentric cylinders rotating at different angular velocities. This instability occurs when the destabilizing effect of the centrifugal force overcomes viscous dissipation. Lord Rayleigh [1] developed an analogy with the Rayleigh-Bénard problem and predicted that for an inviscid fluid, the Taylor-Couette instability cannot occur if the square of the circulation increases monotonically with the radial distance. This configuration is then referred to as *Rayleigh-stable*, in opposition to the *Rayleigh-unstable* regime in which the angular momentum density decreases with the radial distance. Applying a temperature difference between the two cylinders provides a radial density stratification. The rotation of the cylinders gives rise to the centrifugal acceleration which acts on this stratification. The resulting force called *centrifugal buoyancy* can change the stability conditions of the circular Couette flow. To focus on the effect of the centrifugal buoyancy, many authors investigated this problem theoretically in weightless environments. The centrifugal buoyancy destabilizes the flow when the density decreases with the radial distance and has a stabilizing effect in the case of opposite density stratification. The effect of the centrifugal buoyancy can be theoretically derived in the form of a generalized Rayleigh criterion [2–4]. This generalized Rayleigh criterion is similar to the condition presented by Lin [5] using the arguments of von Kármán. The criterion states that the flow remains stable if the product of the density and the square of the circulation increases with the radial distance. Yih [6] improved Lin's stability criterion by

*innocent.mutabazi@univ-lehavre.fr

including viscosity. He performed a linear stability analysis of a circular Couette flow of a viscous fluid with a radial density gradient and highlighted the dual role of the fluid viscosity. On the one hand, the viscosity of a fluid tends to dissipate kinetic energy and therefore stabilizes the flow. On the other hand, because the viscosity forces a displaced particle of fluid to adjust its circulation to that of its new surrounding, the stabilizing effect of outward increase of circulation is diminished. This makes the generalized Rayleigh criterion fail for rotation regimes close to the boundary between Rayleigh-stable and Rayleigh-unstable regimes. Yih's extended criterion of flow stability [6] is that both the density and the square of the circulation must increase with the radial distance.

Many authors studied the stability of Rayleigh-unstable regimes with a radial density gradient [7–14]. These studies underline the rich variety of unstable flows regarding their spatial and temporal structures which depend on the fluid properties and on the curvature of the system. In the Rayleigh-stable regime, the case of solid body rotation [15–18] was widely studied due to its numerous applications in geophysical and atmospheric flows. The Keplerian regime has also been intensely investigated since it is a model for thin accretion disks in astrophysics. The Keplerian rotation, in which the centrifugal acceleration and the central gravitational acceleration are balanced, is characterized by the angular velocity proportional to the radial distance to the power $2/3$. In a Taylor-Couette system, the flow in this rotation regime is realized approximately by cylinders rotating such that the ratio of the angular velocities is proportional to the radius ratio to the power $2/3$. This linearly stable flow is usually coupled with magnetic and gravitational effects [19–21], but the thermohydrodynamic effect associated with the centrifugal acceleration is often neglected. As a first approximation, because the considered fluids have a high electrical conductivity and a low thermal diffusivity, the magnetohydrodynamic has a more prominent effect compared to that of centrifugal buoyancy. However, the centrifugal buoyancy may contribute to the stability of protoplanetary disks in low ionization zones [4].

The aim of the present work is to investigate the general role played by the centrifugal buoyancy in a Taylor-Couette system in the special case of Rayleigh-stable regimes. To focus on the effect of centrifugal buoyancy, microgravity conditions are assumed. A one-dimensional analysis of the linearized perturbation equations leads to a criterion for the stability of differentially heated Taylor-Couette systems. This criterion highlights the role played by a dimensionless parameter Λ combining the temperature difference and the fluid diffusion properties. A three-dimensional linear stability analysis is then performed for two hydrodynamically stable regimes: the regime with stationary inner cylinder and the Keplerian regime. To that end, inward heating configuration is considered for various values of radius ratio, temperature difference and diffusion properties of fluid. We will show that the predictions of the one-dimensional model regarding the parameter Λ are confirmed by the three-dimensional linear stability analysis.

In Sec. II, after being introduced, the equations governing the problem are linearized. A one-dimensional formulation of the problem is derived in Sec. III and leads to a condition for this flow to become unstable. Section IV consists of the three-dimensional linear stability analysis of the two Rayleigh-stable regimes: the Keplerian regime and the regime where the inner cylinder is stationary. The results are discussed in Sec. V and a conclusion is given in Sec. VI.

II. PROBLEM FORMULATION

We consider a Newtonian fluid of density ρ, kinematic viscosity ν, and thermal diffusivity κ confined between two coaxial cylinders of infinite length. The inner cylinder of radius R_1 rotates at an angular velocity Ω_1, while the outer one of radius $R_2 = R_1 + d$ rotates at a different angular velocity Ω_2. The temperatures T_1 and T_2 of the inner and outer cylinders are maintained constant. The temperature difference will be denoted by $\Delta T = T_1 - T_2$. Figure 1 shows the geometry of the considered nonisothermal Taylor-Couette system. The Boussinesq approximation can be adopted for Taylor-Couette systems of cylinders rotating at moderate speeds [22]. It consists in keeping the density of fluid constant except in the centrifugal force term. For that term, the density is considered as dependent linearly on the temperature: $\rho(\theta) = \rho_{\text{ref}}[1 - \alpha\theta]$, where α is the thermal expansion

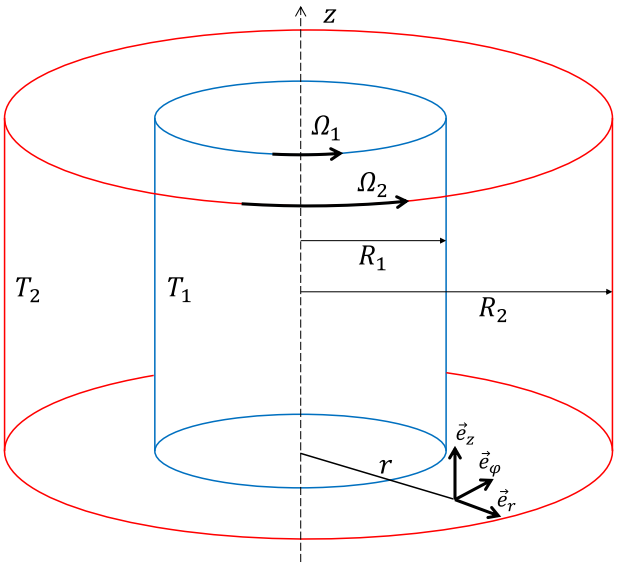

FIG. 1. Schematic representation of the nonisothermal Taylor-Couette system.

coefficient and $\theta = T - T_2$ is the deviation from the reference temperature T_2. The governing laws for the velocity field $\boldsymbol{u} = (u, v, w)$ and the temperature deviation θ are the conservation of mass, momentum, and energy. In the laboratory frame of reference these laws are given by the following equations:

$$\boldsymbol{\nabla} \cdot \boldsymbol{u} = 0, \tag{1a}$$

$$\frac{\partial \boldsymbol{u}}{\partial t} + (\boldsymbol{u} \cdot \boldsymbol{\nabla})\boldsymbol{u} = -\boldsymbol{\nabla}\pi + \nu \Delta \boldsymbol{u} - \alpha\theta \frac{v^2}{r}\boldsymbol{e}_r, \tag{1b}$$

$$\frac{\partial \theta}{\partial t} + (\boldsymbol{u} \cdot \boldsymbol{\nabla})\theta = \kappa \Delta \theta, \tag{1c}$$

in the cylindrical coordinate system $(\vec{e}_r, \vec{e}_\varphi, \vec{e}_z)$ depicted in Fig. 1. A reduced pressure π includes the contribution of the centrifugal acceleration. Imposing no-slip conditions at the cylinder surfaces, the boundary conditions read as follows:

$$\boldsymbol{u} = R_1\Omega_1\boldsymbol{e}_\varphi; \quad \theta = \Delta\mathrm{T}; \quad \text{at} \quad r = R_1, \tag{2a}$$

$$\boldsymbol{u} = R_2\Omega_2\boldsymbol{e}_\varphi; \quad \theta = 0; \quad \text{at} \quad r = R_2. \tag{2b}$$

Seeking for a steady, axisymmetric, and axially invariant solution, we find the base flow which depends on the radial position r only:

$$\Theta = \Delta\mathrm{T}\frac{\ln(r/R_2)}{\ln\eta}, \tag{3a}$$

$$V = -\Omega_1 r\frac{\eta^2 - \mu}{1 - \eta^2} + \frac{\Omega_1 R_1^2}{r}\frac{1 - \mu}{1 - \eta^2}, \tag{3b}$$

where Θ is the temperature and V is the azimuthal flow velocity. We introduced the radius ratio $\eta = R_1/R_2$ and the angular velocity ratio $\mu = \Omega_2/\Omega_1$. The velocity and the temperature fields are decoupled in the base flow.

The set of Eqs. (1) together with the boundary conditions (2) are nondimensionalized using d as the length scale, d^2/ν as the timescale, ν/d as the velocity scale, $(\nu/d)^2$ as the scale of the reduced

TABLE I. Taylor numbers, functions in the boundary conditions, and base flows in the considered two Rayleigh-stable regimes.

	Rotating outer cylinder regime $\Omega_1 = 0$	Keplerian regime $\Omega_1/\Omega_2 = \eta^{-3/2}$
Ta	$\frac{R_2\Omega_2 d}{\nu}\sqrt{\frac{d}{R_2}}$	$\frac{2\eta\Omega_1 d^2(1-\eta^{3/2})}{\nu(1-\eta^2)}$
f_1	0	$\frac{\mathrm{Ta}}{2(1-\eta)}\frac{1-\eta^2}{1-\eta^{3/2}}$
f_2	$\frac{\mathrm{Ta}}{\sqrt{1-\eta}}$	$\frac{\mathrm{Ta}\sqrt{\eta}}{2(1-\eta)}\frac{1-\eta^2}{1-\eta^{3/2}}$
$V(r)$	$\frac{\mathrm{Ta}}{\sqrt{1-\eta}(1+\eta)}\left[r-\frac{\eta^2}{(1-\eta)^2 r}\right]$	$\frac{\mathrm{Ta}}{2}\left[\frac{r(\eta^{3/2}-\eta^2)}{\eta(1-\eta^{3/2})}+\frac{\eta}{r(1-\eta)^2}\right]$

pressure and ΔT as the temperature scale. From now on, unless it is specified, all the quantities are dimensionless. The set of Eqs. (1) now reads

$$\boldsymbol{\nabla}\cdot\boldsymbol{u} = 0, \tag{4a}$$

$$\frac{\partial \boldsymbol{u}}{\partial t} + (\boldsymbol{u}\cdot\boldsymbol{\nabla})\boldsymbol{u} = -\boldsymbol{\nabla}\pi + \Delta\boldsymbol{u} - \gamma_a\theta\frac{v^2}{r}\boldsymbol{e}_r, \tag{4b}$$

$$\frac{\partial \theta}{\partial t} + (\boldsymbol{u}\cdot\boldsymbol{\nabla})\theta = \frac{1}{\mathrm{Pr}}\Delta\theta, \tag{4c}$$

where the Prandtl number $\mathrm{Pr} = \nu/\kappa$ and the thermal expansion parameter $\gamma_a = \alpha\Delta\mathrm{T}$ have been introduced. The boundary conditions (2) are now given by

$$\boldsymbol{u} = f_1(\mathrm{Ta},\eta)\boldsymbol{e}_\varphi, \quad \theta = 1, \quad \text{at} \quad r = \eta/(1-\eta), \tag{5a}$$

$$\boldsymbol{u} = f_2(\mathrm{Ta},\eta)\boldsymbol{e}_\varphi, \quad \theta = 0, \quad \text{at} \quad r = 1/(1-\eta), \tag{5b}$$

where the Taylor number Ta represents the ratio of the characteristic time of viscous dissipation to the characteristic time associated with the centrifugal acceleration. In the present study, the rotation ratio μ will be fixed to particular values of two Rayleigh-stable regimes: $\mu \to \infty$ for the Rotating Outer Cylinder (ROC) regime and $\mu = \eta^{3/2}$ for the Keplerian regime. Depending on the rotation regime, different expressions of the functions f_1 and f_2 are employed in the boundary conditions (5). In addition, we adopt different definitions of the Taylor number depending on the considered rotation regimes to better capture the effect of the rotation of one or both cylinders on the flow. The functions f_1 and f_2, the Taylor number, and the base azimuthal velocity are summarized in Table I. The Taylor number is based on the outer cylinder for the ROC regime, and on the mean geometric radius for the Keplerian regime. The temperature profile of the base flow is given for both regimes by

$$\Theta(r) = \frac{\ln[(1-\eta)r]}{\ln\eta}. \tag{6}$$

The temperature gradient $d\Theta/dr$ remains negative. The heating direction is determined by the sign of γ_a. As we consider only inward heating, this parameter is negative. For this study, $\mathrm{Pr} \in [1, 1000]$, $\gamma_a \in [-0.01, 0]$, and the Taylor number Ta will be restricted by a maximum value of 1000 for the validity of the Boussinesq approximation [22].

Aiming to perform the linear stability analysis, we add infinitesimal perturbations to the base state and linearize the resulting equations around the base flow. These perturbations are expanded in normal modes $(u', v', w', \pi', \theta') = (\hat{u}, \hat{v}, \hat{w}, \hat{\pi}, \hat{\theta})\exp[st + in\varphi + ikz] + \text{c.c.}$, where c.c. stands

for complex conjugate. The primed and hatted quantities indicate the perturbation fields and their complex amplitudes, respectively. The temporal growth rate of perturbations s can be a complex number: $s = \sigma + i\omega$, where σ is the real temporal growth rate which discriminates decaying perturbations from marginal and growing ones, and where ω is the frequency of perturbations. The axial wave number k is a real positive quantity since the cylinders are of infinite length. The azimuthal mode number n takes only integer values. The resulting equations for the complex amplitudes of perturbations are

$$\frac{1}{r}D(r\hat{u}) + \frac{in}{r}\hat{v} + ik\hat{w} = 0, \tag{7a}$$

$$\left(s + \frac{inV}{r}\right)\hat{u} - \frac{2V}{r}\hat{v} = -D\hat{\pi} + \Delta\hat{u} - \frac{\hat{u}}{r^2} - \frac{2in}{r^2}\hat{v} - \frac{\gamma_a}{r}(V^2\hat{\theta} + 2\Theta V\hat{v}), \tag{7b}$$

$$\left(s + \frac{inV}{r}\right)\hat{v} + \left(DV + \frac{V}{r}\right)\hat{u} = -\frac{in}{r}\hat{\pi} + \Delta\hat{v} - \frac{\hat{v}}{r^2} + \frac{2in}{r^2}\hat{u}, \tag{7c}$$

$$\left(s + \frac{inV}{r}\right)\hat{w} = -ik\hat{\pi} + \Delta\hat{w}, \tag{7d}$$

$$\left(s + \frac{inV}{r}\right)\hat{\theta} + (D\Theta)\hat{u} = \frac{1}{\mathrm{Pr}}\Delta\hat{\theta}, \tag{7e}$$

where $D = d/dr$ and $\Delta = D^2 + D/r - n^2/r^2 - k^2$. The perturbations satisfy homogeneous boundary conditions on the cylinder surfaces:

$$\hat{u} = \hat{v} = \hat{w} = \hat{\theta} = 0, \quad \text{at } r = \eta/(1-\eta);\ 1/(1-\eta). \tag{8}$$

The last term in the right-hand side of Eq. (7b) is the perturbed centrifugal buoyancy and includes the effect of the base centrifugal acceleration on the perturbed density profile and the effect of the perturbed centrifugal acceleration on the base density profile.

III. ONE-DIMENSIONAL MODEL

The stability of the Couette flow is modified by a density stratification. In particular, the centrifugal buoyancy will stabilize the flow in the outward heating and will destabilize it in the inward heating [3]. An easy way to derive a criterion showing this effect is to use a one-dimensional model. For this model, only the z dependence of the perturbations is retained in the set of Eqs. (7), i.e., $n = 0$ and $D\hat{u} = D\hat{v} = D\hat{\pi} = D\hat{\theta} = 0$. Since the perturbations depend only on the axial position, the perturbation axial velocity w' vanishes because of the continuity equation and the no-slip boundary condition. The set of equations for the perturbations amplitude Eqs. (7) thus reads in the matrix form:

$$\begin{pmatrix} s + \tilde{k}^2 & -2A\Omega & \gamma_a r\Omega^2 \\ D(r^2\Omega)/r & s + \tilde{k}^2 & 0 \\ D\Theta & 0 & s + k^2/\mathrm{Pr} \end{pmatrix} \begin{pmatrix} \hat{u} \\ \hat{v} \\ \hat{\theta} \end{pmatrix} = \begin{pmatrix} 0 \\ 0 \\ 0 \end{pmatrix}, \tag{9}$$

where $\tilde{k}^2 = k^2 + r^{-2}$ is a positive quantity, $\Omega = V/r$ is the local angular velocity, and $A = 1 - \gamma_a\Theta$. The solvability condition of Eq. (9) requires that the determinant of the matrix in Eq. (9) equals zero, and leads to the dispersion relation:

$$(s + \tilde{k}^2)^2\left(s + \frac{k^2}{\mathrm{Pr}}\right) + 4A\Omega^2(1 + \mathrm{Ro})\left(s + \frac{k^2}{\mathrm{Pr}}\right) - 2\gamma_a\Theta\mathrm{Rt}\Omega^2(s + \tilde{k}^2) = 0. \tag{10}$$

We have introduced the Rossby number $\mathrm{Ro} = rD\Omega/(2\Omega)$, and the thermal Rossby number $\mathrm{Rt} = rD\Theta/(2\Theta)$. Because of the Boussinesq approximation, $|\gamma_a| \ll 1$, therefore the condition $A \approx 1$ is

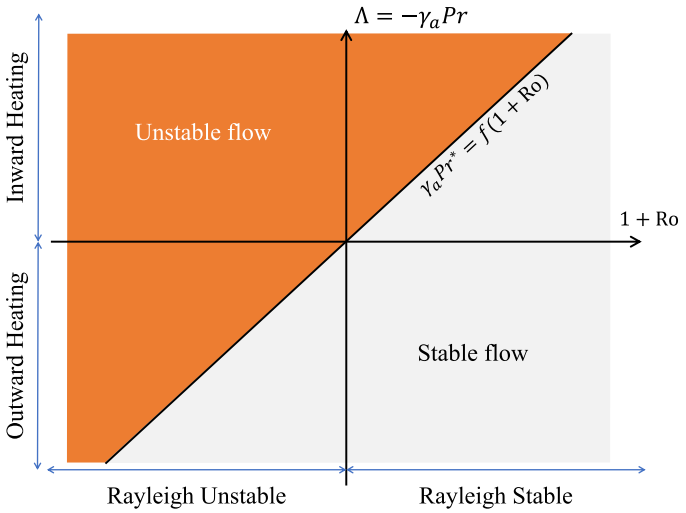

FIG. 2. Schematic representation of the stability of the flow spanned by the parameters $1 + \mathrm{Ro}$ and Λ. The function $f(1 + \mathrm{Ro})$ is defined as the right hand side of the inequality (12).

applied. Assuming the principle of exchange of stability ($s = 0$), we have

$$(2\Omega)^2 \approx \frac{k^2\tilde{k}^4}{\frac{\gamma_a \mathrm{Pr}\Theta}{2}\tilde{k}^2\mathrm{Rt} - k^2(1+\mathrm{Ro})}. \tag{11}$$

For the considered regimes, the thermal Rossby number Rt varies as function of r but remains negative. In the isothermal case ($\gamma_a = 0$) the right hand side of Eq. (11) is positive if $1 + \mathrm{Ro} < 0$. This corresponds to the Rayleigh-unstable flow. In nonisothermal cases, the positivity of the right hand side of Eq. (11) leads to the criterion for the occurrence of an instability:

$$\Lambda = -\gamma_a \mathrm{Pr} > \frac{2(1+\mathrm{Ro})}{\Theta(-\mathrm{Rt})}\frac{k^2}{\tilde{k}^2}. \tag{12}$$

If this inequality holds at any radial distance, an instability would develop. The centrifugal buoyancy parameter Λ is positive if the temperature difference is negative.

An important indication of the criterion (12) is that for any rotation regime, the flow stability would be determined by the parameter γ_aPr. This parameter was used by Walovit *et al.* [7] in a slightly different form which included the curvature of the cylindrical annulus. It corresponds to the ratio between a Rayleigh number based on the centrifugal acceleration and the square of the Taylor number. Styles and Kagan [23] also used the same parameter and named it the temperature drop parameter. Meyer *et al.* [3] remarked that the temperature drop parameter unified the stability conditions obtained for different Pr and γ_a for stationary modes. A schematic representation of the flow stability is shown in Fig. 2 for a given radial position.

In outward heating ($\Lambda < 0$), for Rayleigh-stable flows ($1 + \mathrm{Ro} > 0$) the inequality (12) is never satisfied as the right-hand side of Eq. (12) takes a positive value. In that case both the centrifugal force and the centrifugal buoyancy have stabilizing effects. However, in the case of Rayleigh-unstable flows ($1 + \mathrm{Ro} < 0$), the inequality is satisfied unless γ_aPr exceed certain values so that the stabilizing effect of the centrifugal buoyancy overcomes the destabilizing effect of the centrifugal force. In inward heating ($\Lambda > 0$), Rayleigh-unstable regimes always satisfy the inequality, while Rayleigh-stable regimes can be destabilized by the centrifugal buoyancy. This argument validates the criterion proposed by Yih [6] who found that the viscosity tends to weaken the effect of the stable stratification of angular momentum on a fluid particle pushed outside of equilibrium.

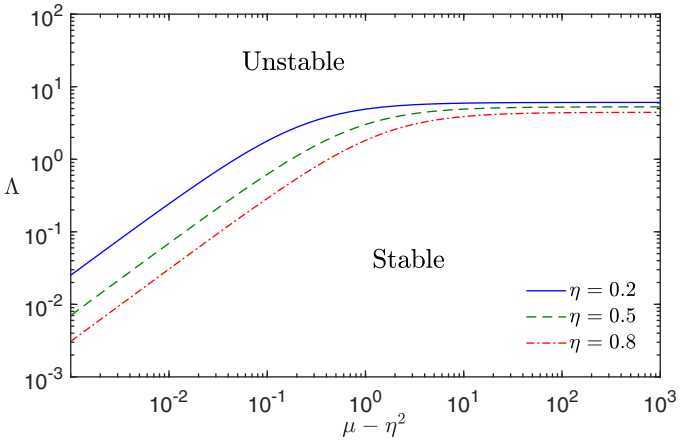

FIG. 3. Evolution of the stability criterion Λ^* as function of $\mu - \eta^2$ for various η. The condition obtained by the one-dimensional model Eq. (13) reveals that the value Λ must be above a certain value Λ^* to make the flow unstable.

When the radial position equals the geometric mean radius $\bar{r} = \sqrt{\eta}/(1-\eta)$, we have $1 + \mathrm{Ro} = (\mu - \eta^2)/[(1-\eta)(\mu+\eta)]$, $\Theta = 1/2$ and $\mathrm{Rt} = 1/\ln\eta$. The inequality (12) can then be written

$$\Lambda > \Lambda^* = B(k,\eta)\frac{\mu-\eta^2}{(1-\eta)(\mu+\eta)}\ln(\eta^{-1}), \tag{13}$$

where $B = 4k^2[k^2 + (1-\eta)^2/\eta]^{-1}$ is a positive coefficient. Counter rotating regimes of Taylor-Couette system are Rayleigh-unstable, but only within a zone between the inner cylinder and the nodal cylindrical surface where the base velocity vanishes [24]. Here the velocity vanishes at the mean geometric radius when $\mu = -\eta$, leading to a discontinuity of Λ^* at that particular position. The choice of this particular radius to derive Eq. (13) is thus not convenient for counter-rotating regimes. For $\mu > -\eta$, the function Λ^* is an increasing function of $\mu - \eta^2$.

Keeping η and k at fixed values, the parameter $\Lambda^* < 0$ for $-\eta < \mu < \eta^2$, meaning that the flow of these rotation regimes are always potentially unstable in inward heating, and can be stabilized in outward heating. When $\mu > \eta^2$ the rotation regime is Rayleigh stable, and in that case, inward heating can destabilize the flow. The condition (13) is shown in Fig. 3 for various radius ratios η and for mode with $k = \pi$. The quantity Λ^* equals zero at $\mu = \eta^2$ and increases with increasing μ. For a given rotation regime, increasing the radius ratio destabilizes the flow. For large values of μ, the parameter Λ^* becomes dependent only of the radius ratio. Overall, the remarkable result simply relies on the fact that for a given curvature of the cylindrical annulus and for a given rotation regime, there exists a value of Λ^* below which the Rayleigh-stable flow cannot be destabilized due to the centrifugal buoyancy. The coupling between thermal and dissipative effects plays a primary role in characterizing the stability of nonisothermal Taylor-Couette systems.

IV. GENERAL 3D CASE

To destabilize a Rayleigh-stable circular Couette flow by applying a temperature difference between the two cylinders, we must have $\gamma_a < 0$, which will be assumed from now on. The equations for the complex amplitude (7) are discretized using the Chebyshev spectral collocation method and completed by the boundary conditions (8). The highest order of considered Chebyshev polynomials was set from 13 to 21 to ensure the convergence, depending on the radius ratio. The resulting generalized eigenvalue problem, written in the matrix form, was solved by the QZ

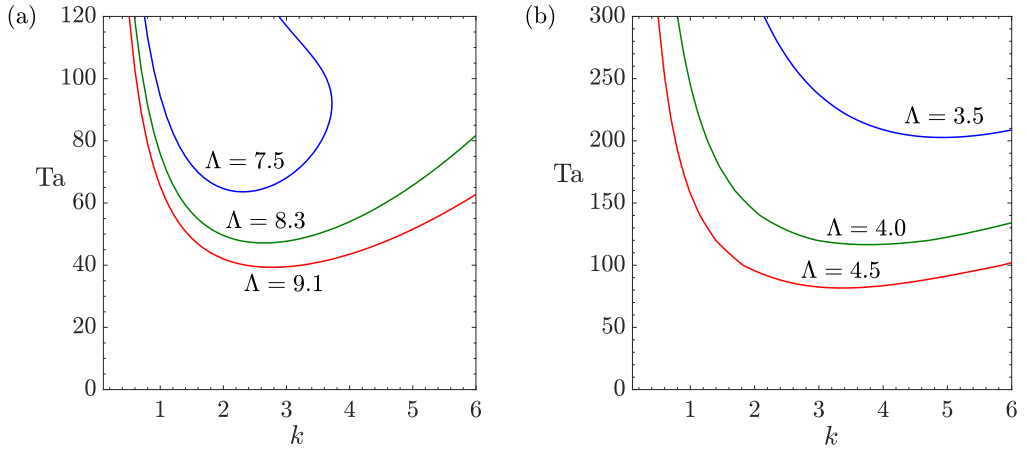

FIG. 4. Marginal stability curves ($\sigma = 0$) in the (k, Ta) plane for various Λ, and for different values of η (a) $\eta = 0.2$ and (b) $\eta = 0.9$ in the ROC regime. The critical parameters corresponding to each marginal curves of (a) and (b) are given in Table II.

decomposition. Solving numerically the eigenvalue problem gives us eigenvalues s for a given set of parameters (η, Pr, γ_a, Ta, n, k). A marginal stability state is obtained when the real part of, at least, one eigenvalue changes the sign from negative to positive. Marginal stability curves are plotted in the (k, Ta) plane for a given set of control parameters (η, Pr, γ_a). The global minimum of marginal stability curves obtained for different azimuthal wave numbers n gives us the critical conditions (Ta_c, n_c, k_c, ω_c).

A. Rotating outer cylinder regime

When only the outer cylinder is rotating, it is found that the critical modes are axisymmetric ($n_c = 0$) and stationary ($\omega_c = 0$). Figure 4 shows the behavior of the marginal stability curves in the (k, Ta) plane for several values of Λ. These curves highlight the behavior of the critical wave number with the variation of Λ for small and large radius ratios. For $\eta = 0.2$, the unstable area, above the marginal curve becomes wider and shifts downward to the right with increasing Λ. For large η (=0.9), the unstable region does not change in shape and shifts downward to the left with increasing Λ.

Although the critical conditions depend on γ_a and Pr, we found that the parameter Λ incorporates the effects of these parameters and allows a unified description. Two systems with a given geometry will exhibit the same threshold Ta_c if they are characterized by the same value of Λ (see Table III). Figure 5 shows the behavior of the critical Taylor number [Fig. 5(a)] and of the critical wave number [Fig. 5(b)] as functions of the centrifugal buoyancy parameter Λ for various values of the radius

TABLE II. Critical parameters for chosen values of Λ in the wide gap ($\eta = 0.2$) and small gap ($\eta = 0.9$) Taylor-Couette flow in the ROC regime for Pr = 1000.

$\eta = 0.2$			$\eta = 0.9$		
Λ	Ta_c	k_c	Λ	Ta_c	k_c
7.5	63.58	2.309	3.5	202.6	4.925
8.3	47.13	2.642	4.0	116.14	3.760
9.1	39.31	2.772	4.5	81.38	3.361

TABLE III. Critical Taylor number and critical wave number for various radius ratios, Prandtl numbers, and thermal expansion parameter.

ROC regime						Keplerian regime					
η	Pr	$-\gamma_a$	Λ	Ta_c	k_c	η	Pr	$-\gamma_a$	Λ	Ta_c	k_c
0.2	700	0.01	7	95.591	1.664	0.2	300	0.01	3	90.169	3.165
0.2	1000	0.007	7	94.752	1.679	0.2	1000	0.003	3	90.043	3.165
0.2	800	0.01	8	51.696	2.557	0.2	800	0.01	8	43.400	3.169
0.2	1000	0.008	8	51.622	2.557	0.2	1000	0.008	8	43.396	3.169
0.5	500	0.01	5	139.139	4.235	0.5	200	0.01	2	48.097	3.127
0.5	1000	0.005	5	137.002	4.139	0.5	1000	0.002	2	48.051	3.127
0.5	800	0.01	8	36.234	3.079	0.5	800	0.01	8	20.391	3.129
0.5	1000	0.008	8	36.214	3.079	0.5	1000	0.008	8	20.390	3.129
0.8	400	0.01	4	142.272	4.186	0.8	100	0.01	1	33.469	3.118
0.8	1000	0.004	4	141.052	3.248	0.8	1000	0.001	1	33.448	3.118
0.8	800	0.01	8	35.708	3.156	0.8	500	0.01	5	13.492	3.118
0.8	1000	0.008	8	35.688	3.156	0.8	1000	0.005	5	13.491	3.118

ratio. The threshold Ta_c decreases with Λ and converges to zero asymptotically. For a given value of Λ, the curvature of the cylindrical annulus has a stabilizing effect. Depending on the radius ratio, there is an asymptotic value of Λ where the critical Taylor number tends to infinity and below which the thermal instability cannot occur. This limit decreases with increasing η. For $\eta = 0.5$ and

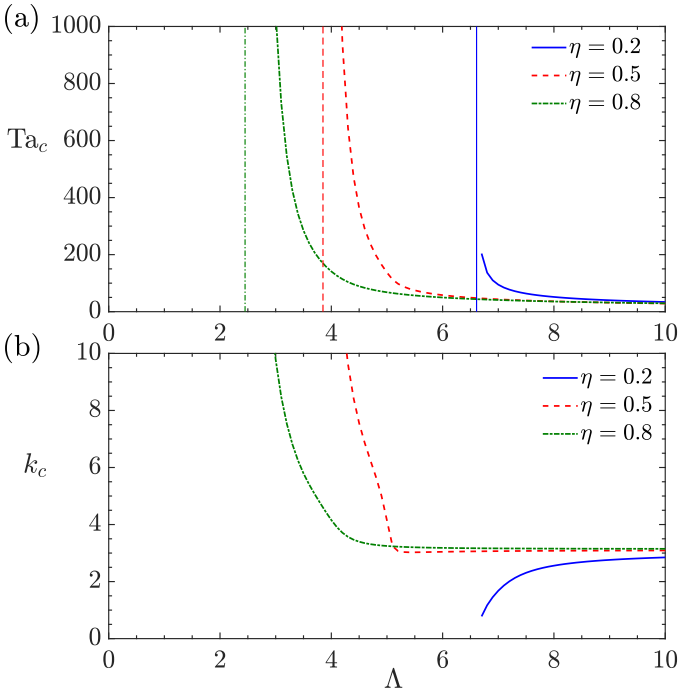

FIG. 5. Variation of the critical parameters with $\Lambda = -\gamma_a \mathrm{Pr}$ in the ROC regime for different η: (a) Taylor number and (b) wave number. For each values of η, a vertical line shows the value Λ^* of Λ below which the flow cannot destabilize; $\Lambda^* = 6.61, 3.85, 2.45$ for $\eta = 0.2, 0.5, 0.8$, respectively.

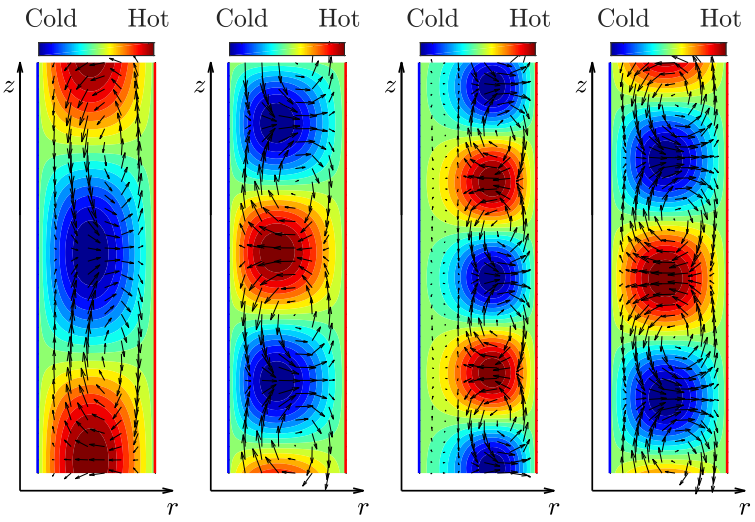

(a) $\eta = 0.2$,	(b) $\eta = 0.2$,	(c) $\eta = 0.5$,	(d) $\eta = 0.5$,
$\gamma_a = -0.007$,	$\gamma_a = -0.01$,	$\gamma_a = -0.005$,	$\gamma_a = -0.01$,
$\mathrm{Ta}_c = 89.63$,	$\mathrm{Ta}_c = 33.67$,	$\mathrm{Ta}_c = 130.63$,	$\mathrm{Ta}_c = 28.43$,
$k_c = 1.773$	$k_c = 2.854$	$k_c = 3.860$	$k_c = 3.091$

FIG. 6. Eigenfunctions at critical conditions in the ROC regime for Pr = 1000 and for different values of η and γ_a.

$\eta = 0.8$ the critical wave number decreases with increasing Λ, but for $\eta = 0.2$ we observed the opposite behavior [Fig. 5(b)].

The eigenfunctions for the perturbation velocity field and for the perturbation temperature at the critical states are illustrated in Fig. 6. The radial velocity perturbation and the temperature perturbation are in anti-phase, which means that a fluid particle traveling from the hot outer cylinder to the cold inner one passes through a high temperature zone while a fluid particle moving in the opposite direction passes through a low temperature zone. For $\eta = 0.2$ the critical wave number is small for small values of Λ and we can see in Fig. 6(a) that large vortices occupy the whole space in the gap. The wavelength decreases when increasing Λ until their axial extension becomes of about the gap size [Fig. 6(b)]. In Fig. 6(c) the vortices observed for $\eta = 0.5$ and for a small value of Λ are shown. The critical wave number is large and we can observe that the vortices are located close to the outer cylinder. The increase of Λ increases the critical wavelength for vortices to occupy the whole gap between the cylinders.

B. Keplerian regime

As in the ROC case, the stability of the Keplerian regime in inward heating can be described conveniently in terms of the centrifugal buoyancy parameter Λ (see Table III). Critical modes are also found to be axisymmetric and stationary. Figure 7 shows the critical parameters variation as function of Λ. The critical Taylor number decreases with increasing Λ and asymptotically tends to zero. The larger the curvature is, the more stable the flow gets. For a fixed radius ratio, there is a limit value Λ^* of Λ below which the flow cannot be destabilized. This limit decreases when increasing the radius ratio and has smaller values than those of the ROC regime. For all the studied

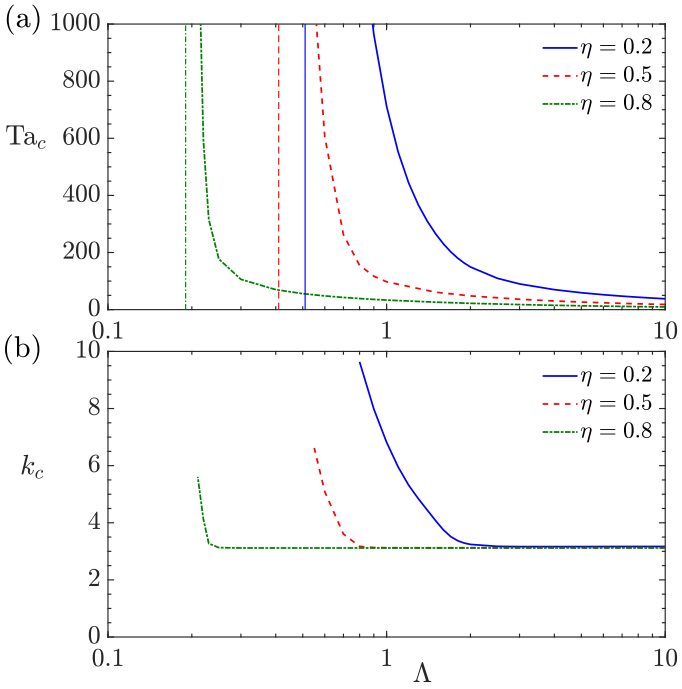

FIG. 7. Variation of the critical parameters with Λ in the Keplerian regime for different η: (a) Taylor number and (b) wave number. For each value of η, a vertical line shows the value Λ^* of Λ below which the flow cannot destabilize; $\Lambda^* = 0.51, 0.41, 0.19$ for $\eta = 0.2, 0.5, 0.8$, respectively.

radius ratios, the critical wave number decreases toward a constant with increasing Λ, which is independent of the radius ratio.

C. Description using the Ginzburg-Landau equation

At the onset of convection the critical modes are stationary and axisymmetric and have a finite wave number. The behavior of the amplitude of perturbation A in the weakly nonlinear regime can thus be described by the Ginzburg-Landau equation [25]:

$$\tau_0 \frac{\partial A}{\partial t} = \epsilon A + \xi_0^2 \frac{\partial^2 A}{\partial z^2} - l|A|^2 A, \tag{14}$$

where $\epsilon = \mathrm{Ta}/\mathrm{Ta}_c - 1$ is the bifurcation parameter. The constants τ_0 and ξ_0 represent the characteristic time and the coherent length of the perturbations, respectively. The characteristic time relates to the time needed for the perturbation flow to be saturated, while the coherent length corresponds to the distance needed for the amplitude to heal from a perturbation suppression, e.g., at a lid of the Taylor-Couette system. These two quantities can be derived from the linear stability analysis by the following formulas:

$$\tau_0 = \left[\mathrm{Ta}_c \left(\frac{\partial \sigma}{\partial \mathrm{Ta}}\right)_c\right]^{-1}, \quad \xi_0^2 = -\frac{\tau_0}{2}\left(\frac{\partial^2 \sigma}{\partial k^2}\right)_c. \tag{15}$$

The Landau constant l determines the nature of the bifurcation from the base flow and cannot be derived from a linear perturbation analysis. It can be determined from a weakly nonlinear analysis or direct numerical simulations [14].

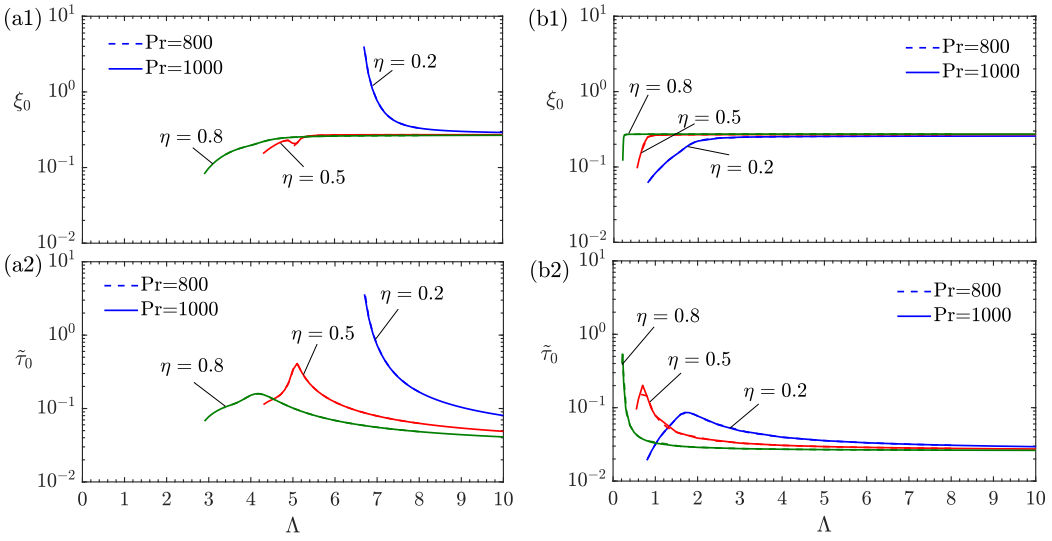

FIG. 8. Variation of the coefficients of the Ginzburg-Landau equation with Λ for various η and various Pr in (a) the rotating outer cylinder regime and (b) the Keplerian regime.

The variations of ξ_0 and $\tilde{\tau}_0 = \tau_0/\mathrm{Pr}$ with the parameter Λ are shown in Fig. 8. For the ROC regime of rotation [Fig. 8(a)], the coherent length decreases with the increase of Λ for $\eta = 0.2$. This behavior is associated with the wave number of the modes, which diminishes when Λ is decreased [Fig. 5(b)]. Modes with wavelength larger than the gap size need more distance for amplitude modulation. The opposite behavior can be seen for $\eta = 0.5$ and $\eta = 0.8$. For these cases with intermediate and small gaps, the wavelength of the modes increases with increasing Λ, and the associated coherent length also increases. The characteristic time $\tilde{\tau}_0$ decreases with increasing Λ for $\eta = 0.2$, but for larger radius ratios, $\tilde{\tau}_0$ first increases with Λ, reaches a maximum value, and then decreases. For the Keplerian rotation regime, the wave number decreases with Λ, and the associated coherent length also decreases with increasing Λ [Fig. 8(b)]. The variation of the characteristic time has a similar behavior to what observed in the ROC regime, i.e., $\tilde{\tau}_0$ increases until it reaches a maximum value, and then starts to decrease with Λ.

For both rotation regimes, at a fixed value of Λ, the Prandtl number has no influence on the coherent length, nor on the characteristic time $\tilde{\tau}_0$. For large Λ and for a given radius ratio, the coherent length converges to a constant value between $1/4$ and $1/3$ of the gap size. This constant slightly diminishes with increasing η and is dependent on the rotation regime. The characteristic time τ_0 varies linearly with the Prandtl number, as in the classical Rayleigh Bénard instability [26,27]. Overall, the observed invariance of ξ_0 and $\tilde{\tau}_0$ to the variation of Pr is an additional indication of the important role played by the parameter Λ.

D. Energy analysis

An energy analysis is used to gain a better understanding of the instability mechanism in the heated Rayleigh-stable Couette system. Multiplying Eqs. (7b)–(7d) by u', v', and w', respectively, and summing the resulting equations leads to the equation for the kinetic energy density of perturbed flow. Integrating over the whole fluid volume, we have

$$\frac{dK}{dt} = W_{\mathrm{Sh}} + W_{\mathrm{Bu}} - D_v, \tag{16}$$

where K is the kinetic energy, W_{Sh} is the power performed by the shear stress, W_{Bu} is the power performed by the centrifugal buoyancy, and D_v is the rate of viscous dissipation. These terms are

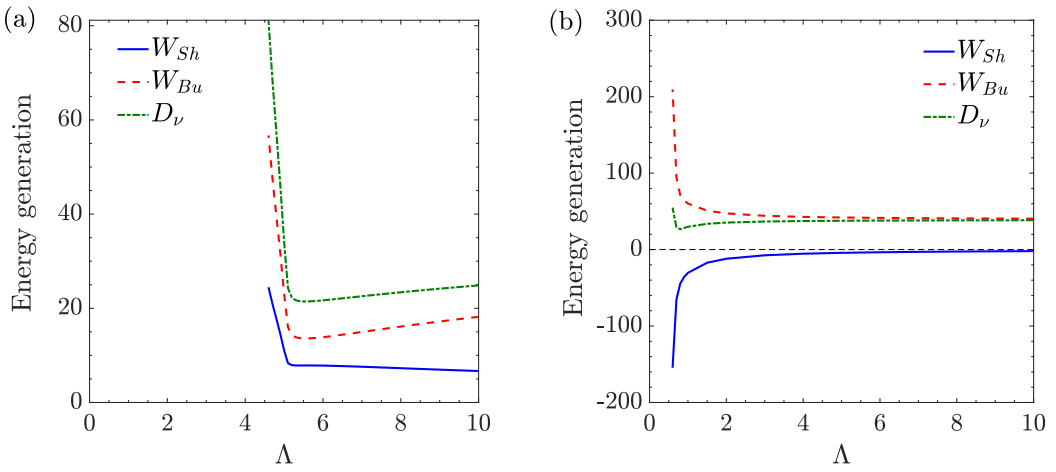

FIG. 9. Power terms as function of Λ for $\eta = 0.5$ and for (a) the ROC regime and (b) the Keplerian regime.

given by

$$K = \int \frac{\boldsymbol{u}'^2}{2} dV, \quad W_{\mathrm{Sh}} = -\int u'v'r\frac{d\Omega}{dr} dV,$$
$$W_{\mathrm{Bu}} = -\gamma_a \int \frac{u'(V^2\theta' + V\Theta v')}{r} dV, \quad D_\nu = \int \Phi_\nu dV, \tag{17}$$

where the viscous dissipation function Φ_ν is given by

$$\Phi_\nu = 2\left[\left|\frac{du'}{dr}\right|^2 + \left|\frac{imv'}{r} + \frac{u'}{r}\right|^2 + k^2|w'|^2\right] + \left|r\frac{d}{dr}\left(\frac{v'}{r}\right) + \frac{imu'}{r}\right|^2$$
$$+ \left|\frac{imw'}{r} + ikv'\right|^2 + \left|iku' + \frac{dw}{dr}\right|^2. \tag{18}$$

Figure 9 shows the variation of the powers W_{Sh}, W_{Bu}, and D_ν with the parameter Λ for the two studied rotation regimes. The power given by the centrifugal buoyancy is always positive, which means that in inward heating, this mechanism contributes to the destabilization of the Couette flow. The contribution of the shear stress to the energy generation is more subtle. For the ROC regime, $W_{\mathrm{Sh}} > 0$ and hence the shear stress destabilizes the flow, while for the Keplerian regime $W_{\mathrm{Sh}} < 0$ and so the shear stress stabilizes the flow. In fact, the sign of W_{Sh} is dependent on the sign of the base flow shear rate $rd\Omega/dr$. This shear rate of the base flow is positive for the ROC regime and negative for the Keplerian regime. The growth of perturbations promoted by the centrifugal buoyancy is weakened by the negative shear rate of base flow in the Keplerian regime, and is reinforced by the positive shear rate in the ROC regime. For both regimes, the power performed by the centrifugal buoyancy and the absolute value of the power performed by the shear stress diminishes when increasing Λ. The rate of viscous energy dissipation always balances the other terms since the growth rate of perturbation flows vanishes at critical conditions.

Figure 10 shows the variation of the power rate terms with the parameter η for the two rotation regimes. For the ROC regime, W_{Bu} increases with increasing η for $\eta < 0.2$ and then decreases for $\eta > 0.2$. The power performed by the shear stress W_{Sh} increases with increasing η. Surprisingly, there exists a certain value of η above which $W_{\mathrm{Bu}} < W_{\mathrm{Sh}}$. For $\eta > 0.75$, while the instability is triggered by the centrifugal buoyancy, the shear stress of the base flow becomes the main mechanism for energy transfer to the vortices formed in the annulus. For η approaching 1, the effect of the shear stress even becomes prominent compared to that of the centrifugal buoyancy. The critical Taylor

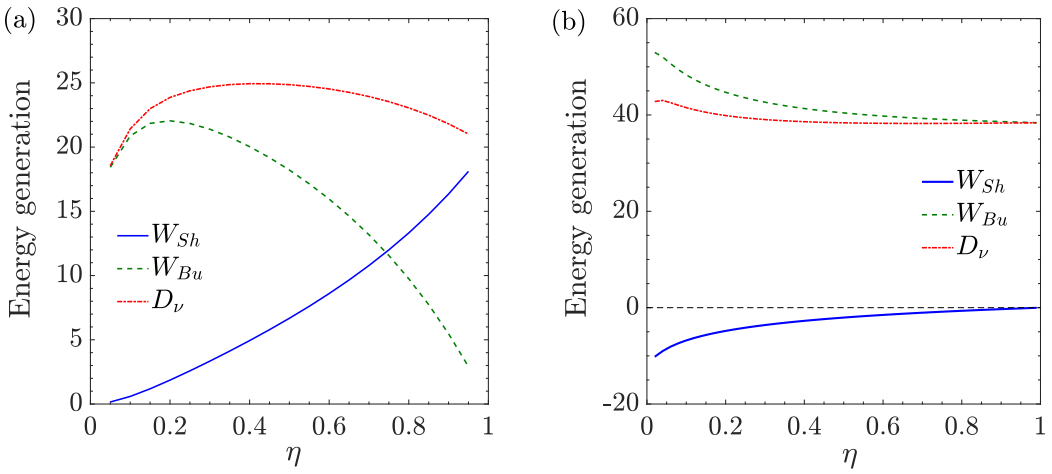

FIG. 10. Power terms as function of η for $\Lambda = 10$ in (a) the ROC regime and (b) the Keplerian regime.

number decreases when the radius ratio is increased, because of the decrease of the power from the centrifugal buoyancy. The shear rate in the ROC regime can be written as

$$r\frac{d\Omega}{dr} = \frac{2\eta^2}{(1+\eta)(1-\eta)^{5/2}}\frac{\mathrm{Ta}}{r^2}. \tag{19}$$

It increases with η, leading to the increase of the power of the shear stress. In the case of the Keplerian regime, W_{Sh} is negative and decreases when the radius ratio is decreased. For large values of Λ and of η, the shear stress does not transfer energy to the perturbations, i.e., $W_{\mathrm{Sh}} = 0$, and the power given by the centrifugal buoyancy becomes constant. The shear rate for the Keplerian regime is given by

$$r\frac{d\Omega}{dr} = \frac{\eta\mathrm{Ta}}{r^2(1-\eta^2)}. \tag{20}$$

The shear stress of the Keplerian regime also increases when the radius ratio is increased, but this time the decrease of the power of the centrifugal buoyancy with η, due to a decrease of the critical Taylor number seems to dominate over that effect.

V. DISCUSSION

A. Lower limit of Λ

As a result of the one-dimensional model (Sec. III), we found that for a given radius ratio and a given rotation regime there exists a lower limit Λ^*. Below this limit, the destabilizing effect of the centrifugal buoyancy in inward heating cannot overcome the stabilizing effects provided by viscous dissipation and, in the Keplerian regime, also by the shear stress. Table IV shows some

TABLE IV. Values of Λ^* calculated from the one-dimensional model (13) for the two studied rotation regimes and for various radius ratios.

η	0.1	0.2	0.3	0.4	0.5	0.6	0.7	0.8	0.9	0.99
ROC	5.62	6.08	5.90	5.60	5.28	4.97	4.70	4.44	4.21	4.02
Kepler.	0.92	1.04	0.95	0.80	0.64	0.49	0.35	0.22	0.11	0.01

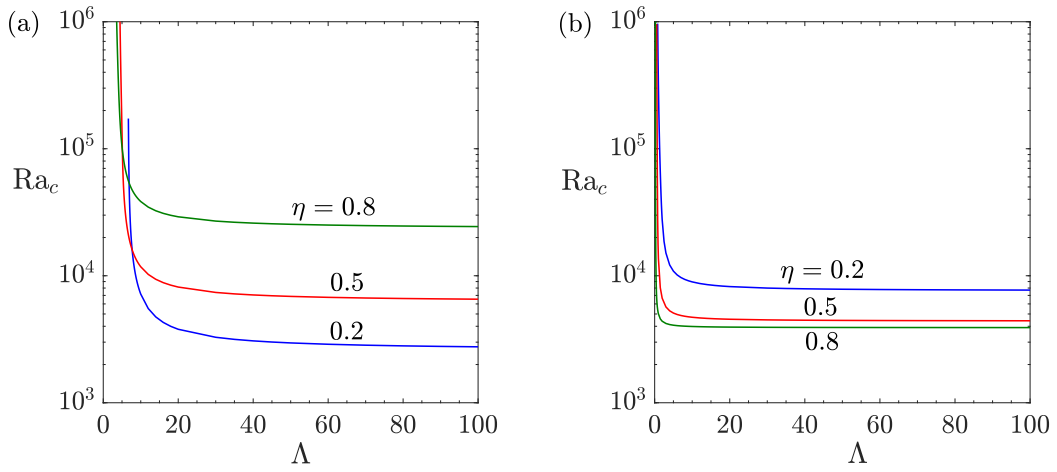

FIG. 11. Variation of the critical Rayleigh number as functions of Λ for $\mathrm{Pr} = 1000$ for various radius ratios in (a) the ROC regime and in (b) the Keplerian regime.

values of Λ^* computed from the instability criterion (13) with $k = \pi$ for the two studied rotation regimes and for various radius ratios. For both rotation regimes, Λ^* is an increasing function of η for $0 < \eta < 0.2$, and decreases with η for $0.2 < \eta < 1$. The ROC regime exhibits much larger Λ^* than the Keplerian regime for all values of η. Figures 5 and 7 indicate the lower limits of Λ for various values of η computed from the three-dimensional linear stability theory. Quantitatively, the one-dimensional model systematically over-estimates Λ^* compared to the three-dimensional calculations. This overestimation can reach 100% and it is attributed to the simplifications made in the one-dimensional model. Nevertheless, the lower limit of Λ calculated from both approaches are of the same order of magnitude and shows the same behavior regarding the influence of the rotation regime and of the radius ratio. Fluids with a Prandtl number of order 10^3 or lower, such as some oil-based ferrofluids [28] may have $\Lambda < \Lambda^*$, where, for instance, $\Lambda^* \sim 1$ in the Keplerian regime. As a results, the centrifugal buoyancy would not be able to destabilize the flow, and an external force field such as thermomagnetic buoyancy [29] would be needed to induce instabilities.

B. Large values of Λ

In Sec. IV D, we saw that the power performed by the the shear stress is a decreasing function of Λ. For sufficiently large values of Λ, W_{Sh} tends to zero. The effect of shear rate can then be neglected. In that case, the centrifugal buoyancy becomes the only force playing a role in flow stability. The system reduces to a Rayleigh-Bénard-like problem where the angular velocity only provides a centrifugal acceleration acting on the density stratification. In a recent article, Kirillov and Mutabazi [4] analyzed the problem both in ROC regime and in the Keplerian regime in the limit of short wavelength of vortices. They derived analytic expressions of the threshold for both regimes and for arbitrary radius ratio. For Λ approaching infinity, their expressions for the critical Taylor number lead to a constant parameter $\mathrm{Ra} = \gamma_a \mathrm{PrTa}^2 / \ln \eta = 1$, independently of the rotation regime, where Ra is a centrifugal Rayleigh number often used to describe the stability of a fluid in a rigidly rotating cylindrical annulus (e.g., in Ref. [18]). The fact that the Rayleigh number becomes constant for large values of Λ indicates that the instability mechanism is analog to that of the Rayleigh-Bénard instability.

Figure 11 shows the variation of the critical Rayleigh number with Λ for various values of η and for both rotation regimes. For large values of Λ, the Rayleigh number tends to a constant. In contrast to the results of Kirillov and Mutabazi [4], the constant value of Ra depends both on the

TABLE V. Values of Λ_∞ above which the shear rate has a negligible influence on the stability. The associated critical Rayleigh number and critical wave number for various radius ratios are given.

ROC regime				Keplerian regime			
η	Λ_∞	Ra_c	k_c	η	Λ_∞	Ra_c	k_c
0.2	420	2590	3.065	0.2	140	7600	3.175
0.5	340	6245	3.111	0.5	70	4390	3.130
0.8	290	23480	3.137	0.8	25	3895	3.118

rotation regime and on the radius ratio. For the ROC regime, this constant increases with η, while for the Keplerian regime, it decreases with η.

Large values of Λ can be realized with highly viscous fluid. For instance in geophysics, magma in the Earth's mantel exhibit a Prandtl number which can be considered as infinite [30]. Some silicone oils have Prandtl numbers of the order of 10^5 [31]. A centrifugal parameter of the order of $\Lambda \sim 10^3$ can therefore be achieved experimentally for a thermal expansion parameter $|\gamma_a| \sim 10^{-2}$. For these large values of Λ, the present analysis predicts that the critical parameters depend only on η and μ. In Table V, the value of Λ_∞ above which the effect of shear rate is negligible is given for both rotation regimes and various values of η. The value of Λ_∞ is defined as the value of Λ when the Rayleigh number reaches its asymptotic value within one percent of difference. Above these values of Λ_∞, the corresponding Rayleigh number given in Table V is considered as constant, and the critical wave number is unchanged. The Keplerian regime exhibits smaller values of Λ_∞ than the ROC regime, and Λ_∞ decreases with η for both regimes.

C. Small gap analysis

Kirillov and Mutabazi [4] investigated the case of axisymmetric perturbations and found, for both ROC and Keplerian rotation regimes, oscillatory critical modes at low Prandtl number and stationary modes above a certain Pr. When only the outer cylinder rotates, the oscillatory axisymmetric modes were not captured by the present linear stability analysis. However, in the Keplerian regime, for $\eta = 0.99$ and $\gamma_a = -0.01$, the oscillatory modes were found as critical modes. The corresponding evolution of the threshold, the critical wave number and the critical frequency with Pr are shown in Fig. 12. The critical modes are axisymmetric and the transition from oscillatory modes to stationary modes occurs at about $\mathrm{Pr} = 1$, which recovers the result of Kirillov and Mutabazi [4] who found oscillatory and stationary modes for $\mathrm{Pr} < 0.98$ and $\mathrm{Pr} > 1.01$, respectively.

VI. CONCLUSION

The stability of Rayleigh-stable flows subject to a radial temperature gradient has been analyzed. A one-dimensional model highlighted the role played by the centrifugal buoyancy parameter $\Lambda = -\gamma_a \mathrm{Pr}$ on the stability of circular Couette flows. Rayleigh-stable flows can become unstable in outward heating configurations and above a certain value of Λ depending on the curvature of the system and on the rotation regime. The existence of this lower limit of Λ was confirmed by a linear stability analysis performed for two distinct rotation regimes: the case where the inner cylinder is at rest while the outer one is rotating and the Keplerian regime. For both regimes, the critical modes take the form of stationary toroidal vortices and for a given radius ratio, the critical Taylor number and the critical wavelength depend only on the parameter Λ. The description of the instability using the Ginzburg-Landau equation also showed that the coherent length of perturbations is constant and that, once measured by the thermal diffusion time d^2/κ, the characteristic time is also constant for fixed values of Λ and η.

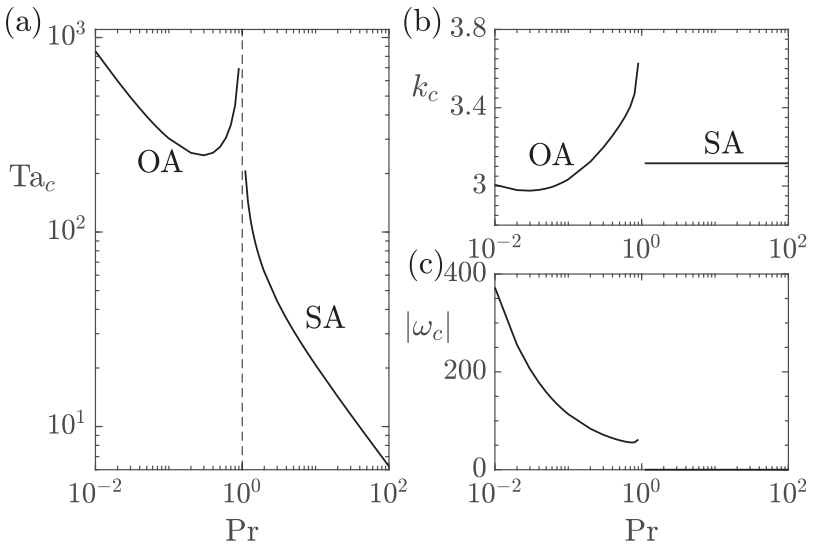

FIG. 12. Variation of the critical parameters as functions of Pr for $\eta = 0.99$ and $\gamma_a = -0.01$ in the Keplerian regime: (a) Taylor number, (b) wave number, and (c) frequency.

Regarding the general mechanism of the instability, the main difference between the rotating outer cylinder regime and the Keplerian regime lies in the opposite sign of their base flow circulations. When only the outer cylinder rotates, the radial shear plays a subtle role. Even though the circulation is stably stratified, the shear stress transfers energy to the perturbation and sustains the vortices. In contrast, in the Keplerian regime, the shear stress drains energy from the perturbations. For large values of Λ and of η, the shear rate plays no role on the stability. The centrifugal buoyancy therefore becomes the only source of energy transfer from the base state to the perturbations.

ACKNOWLEDGMENTS

The present work benefited from the financial support of the French Space Agency (CNES) and the French National Research Agency (ANR) through the program "Investissements d'Avenir" (Grant No. ANR-10 LABX-09-01) LABEX EMC^3 (Project INFEMA).

[1] J. W. Strutt, On the dynamics of revolving fluids, Proc. R. Soc. Lond. A **93**, 148 (1917).
[2] I. Mutabazi and A. Bahloul, Stability analysis of a vertical curved channel flow with a radial temperature gradient, Theor. Comput. Fluid Dyn. **16**, 79 (2002).
[3] A. Meyer, H. N. Yoshikawa, and I. Mutabazi, Effect of the radial buoyancy on a circular Couette flow, Phys. Fluids **27**, 114104 (2015).
[4] O. N. Kirillov and I. Mutabazi, Short-wavelength local instabilities of a circular Couette flow with radial temperature gradient, J. Fluid Mech. **818**, 319 (2017).
[5] C. C. Lin, *The Theory of Hydrodynamic Stability* (Cambridge University Press, New York, 1955).
[6] C. Yih, Dual role of viscosity in the instability of revolving fluids of variable density, Phys. Fluids **4**, 806 (1961).
[7] J. Walowit, S. Tsao, and R. C. Diprima, Stability of flow between arbitrarily spaced concentric cylindrical surfaces including the effect of a radial temperature gradient, J. Appl. Mech. **31**, 585 (1964).
[8] V. M. Soundalgekar, H. S. Takhar, and T. J. Smith, Effect of radial temperature gradient on the stability of viscous flow in an annulus with a rotating inner cylinder, Warme Stoffubertragung **15**, 233 (1981).

[9] H. S. Takhar, T. J. Smith, and V. M. Soundalgekar, Effects of radial temperature gradient on the stability of flow of a viscous incompressible fluid between two rotating cylinders, J. Math. Anal. Appl. **111**, 349 (1985).
[10] H. S. Takhar, M. A. Ali, and V. M. Soundalgekar, Effects of radial temperature gradient on the stability of flow in an annulus with constant heat flux at the inner cylinder: Wide-gap problem, J. Franklin Inst. **325**, 609 (1988).
[11] H. S. Takhar, V. M. Soundalgekar, and M. A. Ali, Effects of radial temperature gradient on the stability of a narrow-gap annulus flow, J. Math. Anal. Appl. **152**, 156 (1990).
[12] C. Kong and I. Liu, The stability of nonaxisymmetric circular Couette flow with a radial temperature gradient, Phys. Fluids **6**, 2617 (1994).
[13] P. M. Eagles and V. M. Soundalgekar, Stability of flow between two rotating cylinders in the presence of a constant heat flux at the outer cylinder and radial temperature gradient-wide gap problem, Heat Mass Transfer **33**, 257 (1997).
[14] C. Kang, A. Meyer, and I. Mutabazi, Radial buoyancy effects on momentum and heat transfer in a circular Couette flow, Phys. Rev. Fluids **2**, 053901 (2017).
[15] F. H. Busse, Thermal instabilities in rapidly rotating systems, J. Fluid Mech. **44**, 441 (1970).
[16] M. Auer, F. H. Busse, and R. M. Clever, Three-dimensional convection driven by centrifugal buoyancy, J. Fluid Mech. **301**, 371 (1995).
[17] F. H. Busse, Centrifugally driven compressible convection, Eur. J. Mech. B **47**, 35 (2014).
[18] C. Kang, A. Meyer, H. N. Yoshikawa, and I. Mutabazi, Numerical study of thermal convection induced by centrifugal buoyancy in a rotating cylindrical annulus, Phys. Rev. Fluids **4**, 043501 (2019).
[19] S. Chandrasekhar, *Hydrodynamic and Hydromagnetic Stability* (Clarendon, Oxford, UK, 1961).
[20] O. N. Kirillov, F. Stefani, and Y. Fukumoto, Local instabilities in magnetized rotational flows: A short-wavelength approach, J. Fluid Mech. **760**, 591 (2014).
[21] A. Child, E. Kersalé, and R. Hollerbach, Nonaxisymmetric linear instability of cylindrical magnetohydrodynamic Taylor-Couette flow, Phys. Rev. E **92**, 033011 (2015).
[22] J. M. Lopez, F. Marques, and M. Avila, The Boussinesq approximation in rapidly rotating flow, J. Fluid Mech. **737**, 56 (2013).
[23] P. J. Stiles and M. Kagan, Stability of cylindrical Couette flow of a radially polarised dielectric liquid in a radial temperature gradient, Physica A **197**, 583 (1993).
[24] C. D. Andereck, S. S. Liu, and H. L. Swinney, Flow regimes in a circular Couette system with independently rotating cylinders, J. Fluid Mech. **164**, 155 (1986).
[25] M. C. Cross and P. C. Hohenberg, Pattern formation outside of equilibrium, Rev. Mod. Phys. **65**, 851 (1993).
[26] M. C. Cross, Derivation of the amplitude equation at the Rayleigh Bénard instability, Phys. Fluids **23**, 1727 (1980).
[27] H. N. Yoshikawa, M. Tadie Fogaing, O. Crumeyrolle, and I. Mutabazi, Dielectrophoretic Rayleigh-Bénard convection under microgravity conditions, Phys. Rev. E **87**, 043003 (2013).
[28] J.-H. Kim, K.-B. Park, and K.-S. Kim, Preparation and characterization of silicone-and-fluorine oil-based ferrofluids, Compos. Res. **30**, 41 (2017).
[29] R. Tagg and P. D. Weidman, Linear stability of radially heated circular Couette flow with simulated radial gravity, Z. Angew. Math. Phys. **58**, 431 (2007).
[30] G. Schubert and D. Bercovicy, *Treatise on Geophysics—Mantle Dynamics* (Elsevier, Amsterdam, 2009).
[31] E. Kaminski and C. Jaupart, Laminar starting plumes in high-Prandtl-number fluids, J. Fluid Mech. **478**, 287 (2003).